Graphical Abstract

To create your abstract, type over the instructions in the template box below.
Fonts or abstract dimensions should not be changed or altered.

Effect of stereochemistry on the catalytic activity of flavopeptides

Leave this area blank for abstract info.

Yukihiro Arakawa*, Nao Takechi, Ken Yamanomoto, Keiji Minagawa, Yasushi Imada*

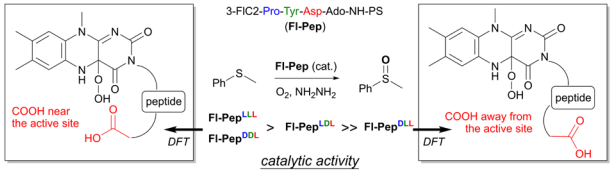

Tetrahedron Letters
journal homepage: www.elsevier.com

Effect of stereochemistry on the catalytic activity of flavopeptides

Yukihiro Arakawa[a], *, Nao Takechi[a], Ken Yamanomoto[a], Keiji Minagawa and Yasushi Imada[a], *

[a]*Department of Applied Chemistry, Tokushima University, Minamijosanjima, Tokushima 770-8506*

ARTICLE INFO

Article history:
Received
Received in revised form
Accepted
Available online

Keywords:
Flavin
Peptide
Aerobic oxidation
DFT calculation

ABSTRACT

The original flavopeptide catalyst, 3-FlC2-L-Pro-L-Tyr-L-Asp-Ado-NH-PS (**Fl-Pep^{LLL}**), and its diastereomers including **Fl-Pep^{DDL}**, **Fl-Pep^{LDL}**, and **Fl-Pep^{DLL}** were synthesized to investigate the correlation between their catalytic activity and stereochemistry. The results and related computations showed the importance of intramolecular hydrogen bonds involving the Asp residue in their 4a-hydroperoxy forms for the catalysis.

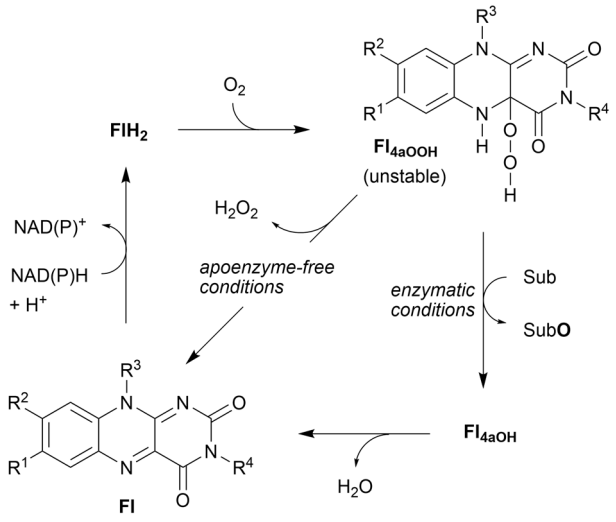

Figure 1. A common view on catalysis under enzymatic conditions and apoenzyme-free conditions for flavin-catalyzed aerobic oxygenation.

The isoalloxazine ring system, **Fl** (Figure 1), is employed as an active center of diverse flavin-dependent enzymes (so-called flavoenzymes) in nature [1]. A notable series of flavoenzymes is flavin-containing monooxygenases that metabolize xenobiotic substrates through the activation of molecular oxygen (O_2) followed by the donation of an oxygen atom to the substrate in mammalian liver (Figure 1, enzymatic conditions). A key active

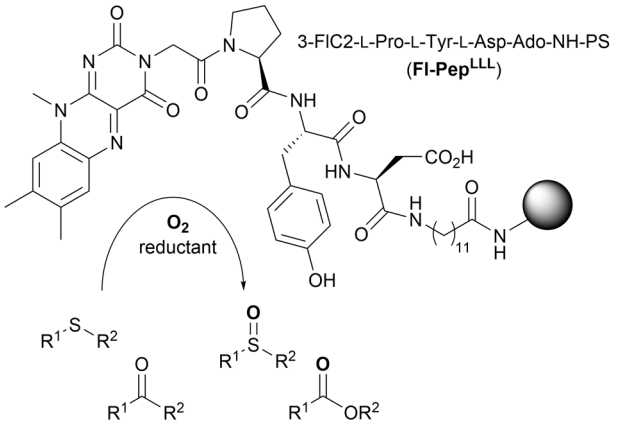

Figure 2. Our previous works on flavin-catalyzed aerobic oxygenation with **Fl-Pep^{LLL}**.

species for the monooxygenation has been recognized to be 4a-hydroperoxy adducts of **Fl**, **Fl$_{4aOOH}$** (Figure 1), which can be properly stabilized by hydrogen bonds under enzymatic conditions to act as an efficient oxidant [2]. Nevertheless, the use of **Fl$_{4aOOH}$** under apoenzyme-free conditions as stoichiometric or catalytic oxidant species was a long-standing challenge due to its substantial lability toward decomposition into **Fl** and H_2O_2 (Figure 1, apoenzyme-free conditions), while a number of approaches with N1- or N5-substituted flavin molecules have so far been studied to overcome this stability issue [3]. In 2017, we succeeded for the first time in using **Fl$_{4aOOH}$** for catalytic aerobic oxygenations under non-enzymatic conditions by means of a designed flavopeptide catalyst, 3-FlC2-L-Pro-L-Tyr-L-Asp-Ado-

* Corresponding author. e-mail: arakawa.yukihiro@tokushima-u.ac.jp

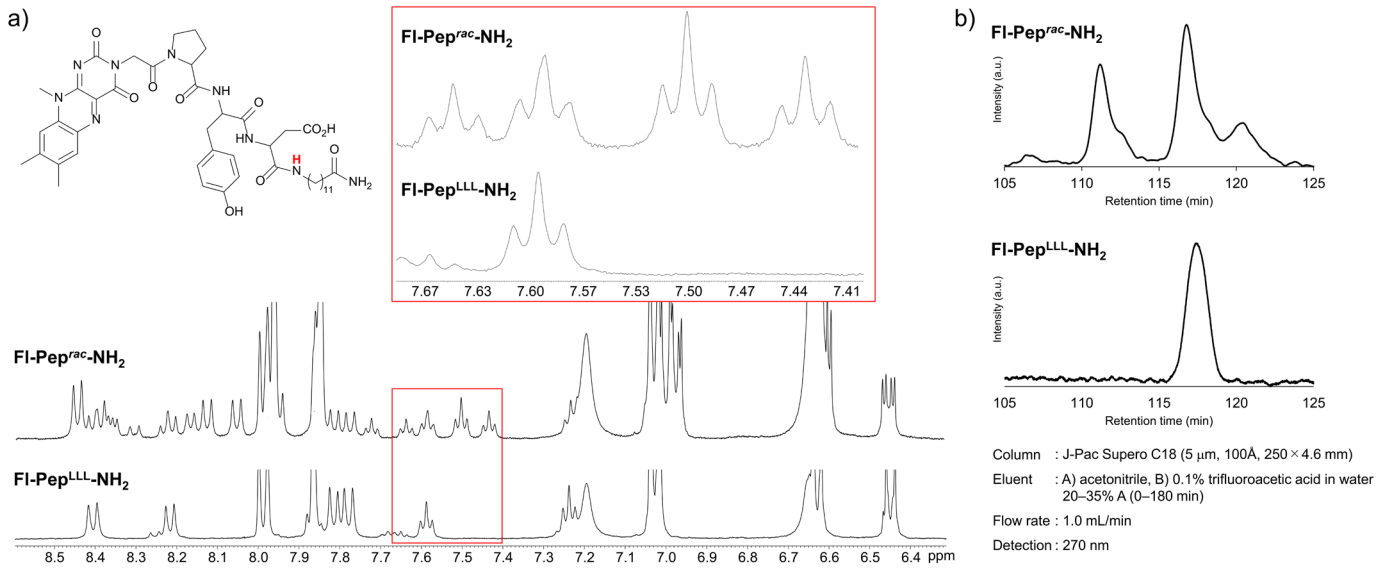

Figure 3. Comparison between **Fl-Pep^{rac}-NH$_2$** and **Fl-Pep^{LLL}-NH$_2$**: (a)^{1}H NMR spectra in DMSO-d_6, (b) RP-HPLC charts.

NH-PS (**Fl-Pep^{LLL}**; 3-FlC2 = lumiflavin-3-acetic acid residue, Ado = 12-aminododecanoic acid residue, Figure 2), consisting of **Fl**, a peptide linker, and polystyrene (PS) resin [4a]. The design of **Fl-Pep^{LLL}** was based on density functional theory (DFT) calculations that predicted the stabilization of the corresponding **Fl$_{4aOOH}$** by the conjugated peptide through intramolecular hydrogen bonds, showing the value of computations for designing peptide-based catalysts. Peptides are attractive tools for molecular catalyst design due to their structural as well as stereochemical diversity [5]. Although all the above components of **Fl-Pep^{LLL}** have experimentally proven to be essential for the catalysis [4], the effect of the stereochemistry of Pro-Tyr-Asp moiety has yet been unexplored.

In the previous reports, **Fl-Pep^{LLL}** was prepared by solid phase peptide synthesis (SPPS) on an aminomethylated PS resin following Fmoc/*t*Bu protocol using *O*-(1*H*-6-chlorobenzotriazole-1-yl)-1,1,3,3-tetramethyluronium hexafluorophosphate (HCTU) as a peptide coupling agent [4]. Since spectroscopic evidence was difficult to obtain due to the compound's insolubility, the quality of **Fl-Pep^{LLL}** was indirectly guaranteed by characterizing its soluble analogue, 3-FlC2-L-Pro-L-Tyr-L-Asp-Ado-NH$_2$ (**Fl-Pep^{LLL}-NH$_2$**) prepared using Rink Amide resin under identical conditions, with 1D and 2D NMR (^{1}H, ^{13}C, COSY, HMBC, HMQC, ROESY) as well as high resolution mass spectroscopy [4a]. Although these NMR analyses did not confirm the presence of epimers, we started this study with an additional analysis by HPLC to get more solid evidence that racemization was not involved in the synthesis of **Fl-Pep^{LLL}** prior to performing the synthesis of its diastereoisomers. As a control, a racemic analogue of **Fl-Pep^{LLL}-NH$_2$**, 3-FlC2-*rac*-Pro-*rac*-Tyr-*rac*-Asp-Ado-NH$_2$ (**Fl-Pep^{rac}-NH$_2$**), was prepared from racemic amino acid ingredients by SPPS on the Rink Amide resin (see supporting information). A ^{1}H NMR spectrum of this racemate showed the existence of four possible diastereomers that were most clearly distinguished with triplet peaks assignable to the amide proton of each Ado residues (Figure 3a, upper). In addition, an acceptable level of diastereoseparation was observed on a C18-reversed phase silica gel for analytical HPLC using a gradient of acetonitrile and 0.1% trifluoroacetic acid in water as a mobile phase (Figure 3b, upper). In contrast, only a single peak among them was obtained both in the ^{1}H NMR spectrum (Figure 3a, lower) and HPLC chart (Figure 3b, lower) for 3-FlC2-L-Pro-L-Tyr-L-Asp-Ado-NH$_2$. These results have convinced us that racemization can be negligible in the SPPS of **Fl-Pep^{LLL}** and its diastereomers (vide infra).

We prepared four enantiomerically pure diastereomers of the flavopeptide including **Fl-Pep^{LLL}** (0.45 mmol g^{-1}), 3-FlC2-D-Pro-D-Tyr-L-Asp-Ado-NH-PS (**Fl-Pep^{DDL}**, 0.49 mmol g^{-1}), 3-FlC2-L-Pro-D-Tyr-L-Asp-Ado-NH-PS (**Fl-Pep^{LDL}**, 0.44 mmol g^{-1}), and 3-FlC2-D-Pro-L-Tyr-L-Asp-Ado-NH-PS (**Fl-Pep^{DLL}**, 0.45 mmol g^{-1}) by the SPPS protocol as follows (Figure 4). Note that the other four possible stereoisomers (**Fl-Pep$^{DDD/LLD/DLD/LDD}$**) are their enantiomers that are therefore not prepared in this study. The construction of peptide moiety was carried out on a commercially available aminomethylated PS resin (1.26 mmol g^{-1}) by repeating a) a coupling of Fmoc amino acids in the presence of HCTU and *N*,*N*-diisopropylethylamine in DMF, which was retried if qualitative Kaiser test [6a] was positive, b) a capping of undetectable residual amino groups on the resin by treating with acetic anhydride in the presence of triethylamine in CH_2Cl_2, and c) a removal of Fmoc group using piperidine in DMF. The resulting peptide intermediates on the resin were reacted with lumiflavin-3-acetic acid (3-FlC2-OH) under identical conditions as a) to attach the flavin moiety on their N-terminus, which was confirmed by qualitative chloranil test [6b], and finally treated with trifluoroacetic acid in CH_2Cl_2 to remove *tert*-butyl groups and give the target flavopeptides.

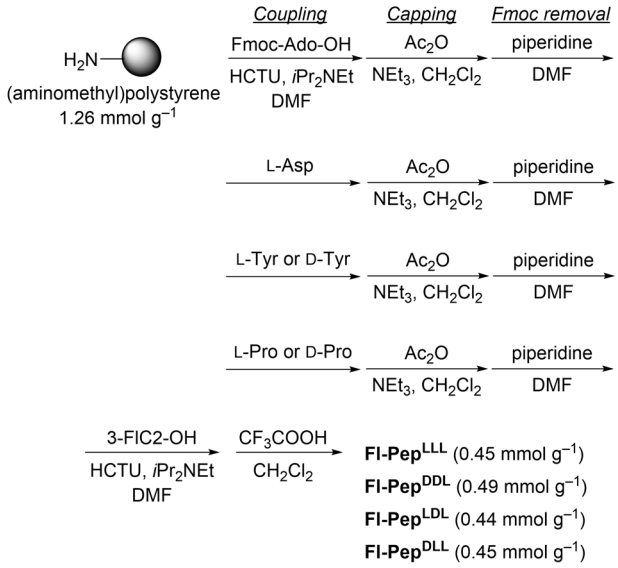

Figure 4. Synthesis of flavopeptides.

We previously reported that the aerobic oxidation of thioanisole proceeded in the presence of 10 mol% of **Fl-Pep^{LLL}** and 1 atm of O_2 and 4 equivalents of hydrazine monohydrate in a 1:1 mixed solvent of 2,2,2-trifluoroethanol (TFE) and 1,2-dichloroethane (DCE) at 25 °C while protected from light to give methyl phenyl sulfoxide in 62% yield after 24 h or 99% yield

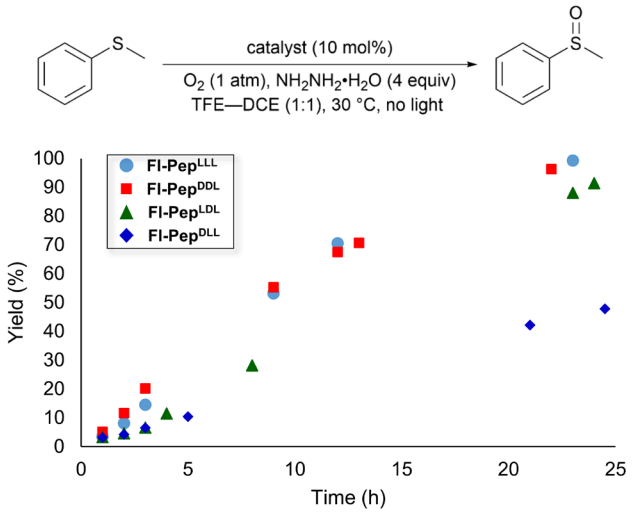

Figure 5. Reaction profiles of catalytic aerobic oxidation of thianisole with flavopeptides.

after 36 h without any side reaction: note that the structural and functional requirements, except stereochemistry, for the catalytic activity of **Fl-Pep^{LLL}** were already established by control experiments using suitable analogues as a catalyst [4a]. To explore the effect of peptide's stereochemistry on the catalysis, the catalytic activities of **Fl-Pep^{LLL}**, **Fl-Pep^{DDL}**, **Fl-Pep^{LDL}**, and **Fl-Pep^{DLL}** were compared in the aerobic oxidation of thioanisole at 30 °C under otherwise identical conditions. Reactions were monitored by gas chromatography analysis to draw their profiles (Figure 5). **Fl-Pep^{LLL}** (light blue circle) and **Fl-Pep^{DDL}** (red square) showed almost the same activity, in which the desired reaction proceeded quantitatively within 24 h. **Fl-Pep^{LDL}** (green triangle) exhibited a slightly lower activity compared to **Fl-Pep^{LLL}** and **Fl-Pep^{DDL}** with a clearer sigmoidal reaction profile. In contrast, **Fl-Pep^{DLL}** (blue rhombus) was much less active and more than half of the substrates were unreacted in 24.5 h. It should be noted that the reaction profile of **Fl-Pep^{DLL}** was also a sigmoid as in other cases, probably because of taking time for **Fl$_{4aOOH}$** to reach its maximum concentration. These results indicate that the stereochemistry of Pro-Tyr-Asp moiety of flavopeptides influences on their catalysis. Unfortunately, the product was racemic in each case.

Fl-Pep^{LLL} was originally designed by predicting the lowest energy structure of the corresponding **Fl$_{4a(R)OOH}$** by means of DFT calculations [4a]. Thereupon, we utilized the same computational tool to rationalize the difference between **Fl-Pep^{LLL}**, **Fl-Pep^{DDL}**, **Fl-Pep^{LDL}**, and **Fl-Pep^{DLL}** in their catalytic activity. For the calculation, 3-FlC2$_{4a(R)OOH}$-L-Pro-L-Tyr-L-Asp-NHMe (**Fl$_{4a(R)OOH}$-Pep^{LLL}-NHMe**), 3-FlC2$_{4a(R)OOH}$-D-Pro-D-Tyr-L-Asp-NHMe (**Fl$_{4a(R)OOH}$-Pep^{DDL}-NHMe**), 3-FlC2$_{4a(R)OOH}$-L-Pro-D-Tyr-L-Asp-NHMe (**Fl$_{4a(R)OOH}$-Pep^{LDL}-NHMe**), and 3-FlC2$_{4a(R)OOH}$-D-Pro-L-Tyr-L-Asp-NHMe (**Fl$_{4a(R)OOH}$-Pep^{DLL}-NHMe**) were supposed. Monte Carlo conformational searches in MMFF were conducted and the resulting conformers with relative potential energy below 10 kJ mol^{-1} and Boltzmann distribution value above 0.02 were extracted as initial structures and recalculated in DFT at B3LYP/6-31G* level to give a few stable conformations for each accounting for 92.5–99.7% of the total Boltzmann weights (Figure 6). Note that these calculations deliberately assume a situation in which solvent molecules are not involved, because of the importance of hydrophobic environments provided by PS resin allowing for the efficient catalysis as previously demonstrated [4]. First of all, their lowest energy structures (at the left end of each row) were compared in terms of the number and mode of intramolecular hydrogen bonds excluding one between CO (i) and NH (i+2) observed in common to favor a γ-turn structure [4a,5d]. Although countable hydrogen bonds between the flavin moiety and the peptide chain were comparable (3–4H bonds), only **Fl$_{4a(R)OOH}$-Pep^{DLL}-NHMe** was dissimilar in how COOH (i+3) was involved; the carboxyl group in **Fl$_{4a(R)OOH}$-Pep$^{LLL/DDL/LDL}$-NHMe** behaved both as a hydrogen bond donor and a hydrogen bond acceptor near the C(4a) position of flavin ring system, while that in **Fl$_{4a(R)OOH}$-Pep^{DLL}-NHMe** provided only one hydrogen bond from away from the active site. As previously proposed, hydrazine may be included by forming a carboxylic acid salt to stabilize/activate the peroxy species in the actual reaction system with **Fl-Pep^{LLL}**, and the resulting oxygen transfer to a substrate is the rate-determining step of the catalysis [4a]. From this viewpoint, **Fl$_{4a(R)OOH}$-Pep$^{LLL/DDL/LDL}$-NHMe** seems to have room for such a hydrazine intervention to keep effective intramolecular interactions (Figure 7a), explaining the relationship **Fl-Pep$^{LLL/DDL/LDL}$** >> **Fl-Pep^{DLL}** in catalytic activity. Based on this theory, the relationship **Fl-Pep^{LLL}** ≈ **Fl-Pep^{DDL}** > **Fl-Pep^{LDL}** in catalytic activity can also be rationalized by looking out over the whole stable structures narrowed down by the calculations (Figure 6). The COOH (i+3) group was ideally involved in the hydrogen bonds of all structures found for **Fl$_{4a(R)OOH}$-Pep$^{LLL/DDL}$-NHMe**. On the other hand, none of the second and subsequent stable structures for **Fl$_{4a(R)OOH}$-Pep^{LDL}-NHMe** contained the ideal involvement of COOH (i+3) in their hydrogen bond interactions, in which the hydroperoxy species could be labile to readily decompose into **Fl-Pep** and H_2O_2 (Figure 7b). These observations demonstrated a reliable correlation between catalytic activities and computational outputs, leading us to conclude that the stereochemistry of flavopeptides could make a difference in the production of **Fl$_{4aOOH}$** in their catalysis.

In summary, we demonstrated that racemization could be no concern in the synthesis of **Fl-Pep^{LLL}** and prepared its diastereomers including **Fl-Pep^{DDL}**, **Fl-Pep^{LDL}**, and **Fl-Pep^{DLL}** in an enantiomerically pure form. The aerobic oxidation of thioanisole was explored by means of these flavopeptides as a catalyst, which revealed the relationship **Fl-Pep^{LLL}** ≈ **Fl-Pep^{DDL}** > **Fl-Pep^{LDL}** >> **Fl-Pep^{DLL}** in catalytic activity. DFT calculations of **Fl$_{4a(R)OOH}$-Pep^{LLL}-NHMe**, **Fl$_{4a(R)OOH}$-Pep^{DDL}-NHMe**, **Fl$_{4a(R)OOH}$-Pep^{LDL}-NHMe**, and **Fl$_{4a(R)OOH}$-Pep^{DLL}-NHMe** disclosed that the stereochemistry of the peptide moiety could significantly influence the mode of intramolecular hydrogen bonds in their stable structures, in which, in particular, the involvement of COOH (i+3) was found to correlate well with the catalytic activity. With the present knowledge and methodologies in hand, we are currently working on the design of flavopeptides as asymmetric catalysts.

Acknowledgments

This work was supported by JSPS KAKENHI (Grant-in-Aid for Scientific Research (C), no. 18K05108).

References and notes

[1] a) T. C. Bruice, Acc. Chem. Res. 13 (1980) 256–262;
b) C. Walsh, Acc. Chem. Res. 13 (1980) 148–155;
c) D. P. Ballou, 'Flavoprotein Monooxygenases' in 'Flavins and flavoproteins', Eds. V. Massey, C. H. Williams, Elsevier: New York, 1982;
d) 'Chemistry and biochemistry of flavoenzymes', Ed. F. Müller, CRC Press: Boston, 1991;
e) R. B. Silverman, Acc. Chem. Res. 28 (1995) 335–342;
f) N. M. Kamerbeek, D. B. Janssen, W. J. H. van Berkel, M. W. Fraaije, Adv. Synth. Catal. 345 (2003) 667–678;
g) 'Flavins-photochemistry and photobiology', Eds. E. Silva, A. M. Edwards, Royal Society of Chemistry: Cambridge, 2006;
h) M. W. Fraaije, D. B. Janssen, 'Biocatalytic scope of Baeyer-Villiger Monooxygenases' in 'Modern biooxidation: enzymes, reactions and applications', Eds. R. D. Schmid, V. B. Urlacher, Wiley-VCH: Weinheim, 2007;
i) M. Insińska-Rak, M. Sikorski, Chem. Eur. J. 20 (2014) 15280–15291;

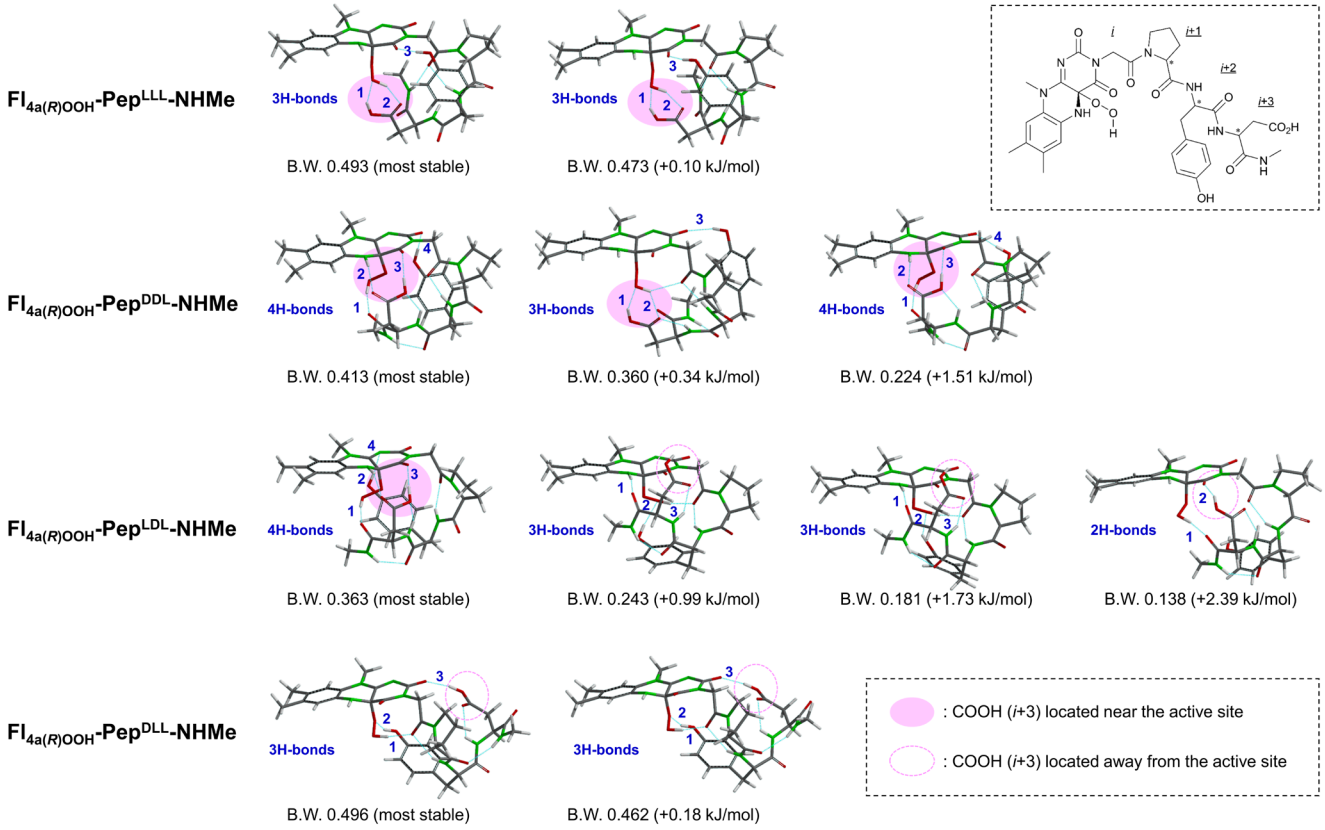

Figure 6. Low energy structures of **Fl$_{4a(R)OOH}$-Pep^{LLL}-NHMe**, **Fl$_{4a(R)OOH}$-Pep^{DDL}-NHMe**, **Fl$_{4a(R)OOH}$-Pep^{LDL}-NHMe**, and **Fl$_{4a(R)OOH}$-Pep^{DLL}-NHMe** estimated by DFT calculations (B.W. = Boltzmann weight)

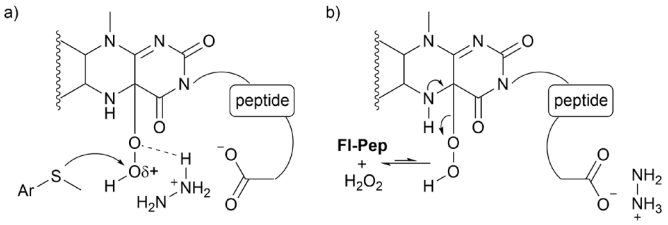

Figure 7. A plausible role of the COOH (*i*+3) of **Fl-Pep** located a) near the active site, b) away from the active site.

j) J. Lee, F. Müller, A. J. W. G. Visser, Photochem. Photobiol. 95 (2019) 679–704.

[2] a) L. L. Poulsen, D. M. Ziegler, J. Biol. Chem. 254 (1979) 6449–6455;
b) V. Massey, P. Hemmerich, Biochem. Soc. Trans. 8 (1980) 246–257;
c) N. B. Beaty, D. P. Ballou, J. Biol. Chem. 255 (1980) 3817–3819.

[3] a) H. Iida, Y. Imada, S.-I. Murahashi, Org. Biomol. Chem. 13 (2015) 7599–7613;
b) R. Cibulka, Eur. J. Org. Chem. (2015) 915–932;
c) G. de Gonzalo, M. W. Fraaije, ChemCatChem 5 (2013) 403–415;
d) Y. Imada, T. Naota, Chem. Rec. 7 (2007) 354–361;
e) F. G. Gelalcha, Chem. Rev. 107 (2007) 3338–3361;
f) J.-E. Bäckvall in 'Modern oxidation methods', Ed. J.-E. Bäckvall, Wiley-VCH: Weinheim, 2004.

[4] a) Y. Arakawa, K. Yamanomoto, H. Kita, K. Minagawa, M. Tanaka, N. Haraguchi, S. Itsuno, Y. Imada, Chem. Sci. 8 (2017) 5468–5475;
b) K. Yamanomoto, H. Kita, Y. Arakawa, K. Minagawa, Y. Imada, Chimia 72 (2018) 866–869.
c) Y. Arakawa, K. Minagawa, Y. Imada, Polym. J. 50 (2018) 941–949.

[5] a) E. A. C. Davie, S. M. Mennen, Y. Xu, S. J. Miller, Chem. Rev. 107 (2007) 5759–5812;
b) H. Wennemers, Chem. Commun. 47 (2011) 12036–12041;
c) J. Duschmale, Y. Arakawa and H. Wennemers, in *Science of Synthesis: Asymmetric Organocatalysis*, Ed. K. Maruoka, Thieme, Stuttgart, 2012, p. 741;
d) A. J. Metrano, A. J. Chinn, C. R. Shugrue, E. A. Stone, B. Kim, S. J. Miller, Chem. Rev. 120 (2020) 11479–11615;
e) K. Akagawa, K. Kudo, Acc. Chem. Res. 50 (2017) 2429–2439.

[6] a) E. Kaiser, R. L. Colescott, C. D. Bossinger, P. I. Cook, Anal. Biochem. 34 (1970) 595–598;
b) T. Vojkovsky, Pept. Res. 8 (1995) 236–237.

Appendix A. Summlementary data

Supplementary data to this article can be found online at https://...